Accepted for Presentation to the IEEE MTT-S Microwave Conference 1998

NONLINEAR CIRCUIT CHARACTERIZATION USING A MULTIRESOLUTION TIME DOMAIN TECHNIQUE (MRTD)

Luca Roselli[1], Emmanouil M. Tentzeris[2], Linda P.B. Katehi[2]
[1] University of Perugia, Perugia, ITALY
[2] Radiation Laboratory, Department of Electrical Engineering and Computer Science
University of Michigan, Ann Arbor, MI 48109–2122, U.S.A.

Abstract- The MRTD scheme is applied to the modeling of nonlinear circuits. Specifically, the implementation of passive and active elements is discussed. The results are compared to those obtained by use of the commercial CADs to indicate considerable savings in memory and computational time.

I Introduction

Recently, the use of multiresolution analysis for the discretization of the time-domain Maxwell's equations has led to the development of the Multiresolution Time Domain Technique (MRTD). This technique has been applied to linear as well as nonlinear propagation problems and has demonstrated savings in time and memory of two orders of magnitude. In addition, the most important advantage of this new technique is its capability to provide a very effective way for space and time adaptive gridding without encountering the problems that the conventional FDTD has to resolve.

In this paper, an algorithm to model nonlinear circuits using the MRTD scheme is proposed and applied to diode problems. As an example, the harmonic analysis of a diode enclosed in a metallic shield and terminated with lumped resistors is performed and a simple stripline mixer circuit using the same diode is analyzed.

II The MRTD scheme

To derive the MRTD scheme, the field components are expanded in a series of cubic spline Battle-Lemarie [1, 2] scaling and wavelet functions in space and pulse functions in time. The MRTD equations are derived by applying the Method of Moments to the Maxwell's equations after inserting the field expansions.

For open structures, the perfectly matched layer (PML) technique can be applied by assuming that the conductivity is given in terms of scaling and wavelet functions instead of pulse functions with respect to space [3]. The MRTD mesh is terminated by a perfect electric conductor (PEC) at the end of the PML region. Unlike the FDTD, where the consistency with the image theory is implicit in the application of the boundary conditions, the entire-domain nature of the wavelet and scaling functions requires an explicit use of the boundary conditions. In particular, image theory has to be applied for the evaluation of the field component coefficients in the vicinity of Perfect Electric and Magnetic Walls. Due to the nature of the Battle-Lemarie expansion functions, the total field is a summation of the contributions from the non-localized scaling and wavelet functions.

III Lumped Elements

Similarly to LE-FDTD technique [4], the basis of the algorithm is given by a particular interpretation of the current density term contained in the $Curl(H)$ Maxwell's equation. Let's assume for the rest of the discussion that all the lumped elements are z-oriented.

$$\epsilon \frac{\partial E_z}{\partial t} = \hat{z} \cdot (\bar{\nabla} \times \bar{H}) + J_c^z \qquad (1)$$

The current term can be considered as the superposition of two separate terms, one coming from the finite conductivity of the medium J_σ^z and the other coming from the presence of a lumped element J_{lu}^z. Eq.(1) leads to the following general updating expression for the E-field S-MRTD (Scaling-functions-based) coefficients:

$$\begin{aligned} \epsilon \frac{{}^{k+1}E^{\phi z}_{l,m,n+\frac{1}{2}} - {}^{k}E^{\phi z}_{l,m,n+\frac{1}{2}}}{\Delta t} &= \hat{z}\cdot(\bar{\nabla}\times\bar{H}) \\ &+ {}_{k+\frac{1}{2}}J^{\phi z}_{l,m,n+\frac{1}{2}} \end{aligned}$$

where an ideal dielectric medium with $\sigma = 0$ has been assumed. The discretization of the last term can be obtained by expressing the constitutive relationship of the related device in terms of electric field and current density (instead of V-I relation as usual).

Since the field components are expanded in pulses in the time-domain, the time discretization of the J-E relation of the lumped devices is straightforward and similar to FDTD.

III.1 Resistor

Assuming that the resistor is z-oriented and a positive voltage (with respect to the z-axis) is applied, we have:

$$V_z = -\Delta z E_z \ , \quad I_z = J_{lu}^z \Delta x \Delta y \qquad .$$

Since the current flow due to a positive voltage is negative with respect to the z-axis, Ohm's Law can be written in the following form:

$$J_{lu}^z = \frac{\Delta z E_z}{R\Delta x \Delta y} \qquad . \tag{2}$$

By discretizing equations 1 and 2 accordingly to the S-MRTD scheme and assuming that no current density is supported by the medium we obtain:

$$\begin{aligned} {}^{k+1}E^{\phi z}_{l,m,n+\frac{1}{2}} &= \frac{B}{C}\,{}^{k}E^{\phi z}_{l,m,n+\frac{1}{2}} + \\ &+ \frac{1}{C\Delta x}\sum_{i=l-9}^{l+8} a(i)_{k+\frac{1}{2}} H^{\phi y}_{i+\frac{1}{2},m,n+\frac{1}{2}} - \\ &- \frac{1}{C\Delta y}\sum_{j=m-9}^{m+8} a(j)_{k+\frac{1}{2}} H^{\phi x}_{l,j+\frac{1}{2},n+\frac{1}{2}} \end{aligned}$$

where

$$B = \frac{\epsilon}{\Delta t} - \frac{\Delta z}{2R\Delta x\Delta y} \ , \quad C = \frac{\epsilon}{\Delta t} + \frac{\Delta z}{2R\Delta x\Delta y} \qquad .$$

III.2 Capacitor

The I-V Law of the capacitor is:

$$I(t) = C\frac{dV(t)}{dt}$$

Expanding the E- and H- components in scaling functions in space and pulses in time and applying the Moments Method, the capacitor can be described by

$$\begin{aligned} {}^{k+1}E^{\phi z}_{l,m,n+\frac{1}{2}} &= {}^{k}E^{\phi z}_{l,m,n+\frac{1}{2}} + \\ &+ \frac{1}{B\Delta x}\sum_{i=l-9}^{l+8} a(i)_{k+\frac{1}{2}} H^{\phi y}_{i+\frac{1}{2},m,n+\frac{1}{2}} - \\ &- \frac{1}{B\Delta y}\sum_{j=m-9}^{m+8} a(j)_{k+\frac{1}{2}} H^{\phi x}_{l,j+\frac{1}{2},n+\frac{1}{2}} \end{aligned}$$

where the coefficient B is given by:

$$B = \frac{\epsilon + C\frac{\Delta z}{\Delta x\Delta y}}{\Delta t} \qquad .$$

III.3 Inductor

The constitutive relation of the inductor is:

$$I(t) = L\int V(t)dt \qquad .$$

Following the same procedure described for the resistor and the capacitor we obtain:

$$\begin{aligned} {}^{k+1}E^{\phi z}_{l,m,n+\frac{1}{2}} &= \frac{C}{A}\,{}^{k}E^{\phi z}_{l,m,n+\frac{1}{2}} - \frac{B}{A}\sum_{i=1}^{k} {}_{i}E^{\phi z}_{l,m,n+\frac{1}{2}} + \\ &+ \frac{1}{A\Delta x}\sum_{i=l-9}^{l+8} a(i)_{k+\frac{1}{2}} H^{\phi y}_{l+\frac{1}{2},m,n+\frac{1}{2}} - \\ &- \frac{1}{A\Delta y}\sum_{j=m-9}^{m+8} a(j)_{k+\frac{1}{2}} H^{\phi x}_{l,j+\frac{1}{2},n+\frac{1}{2}} \end{aligned}$$

where the coefficients A, B, C are given by:

$$A = \frac{\epsilon}{\Delta t} + \frac{\Delta z\Delta t}{2L\Delta x\Delta y} \ , \quad B = \frac{\Delta z\Delta t}{2L\Delta x\Delta y} \ , \quad C = \frac{\epsilon}{\Delta t} \qquad .$$

III.4 Diode with Junction and Diffusion Capacitances

According to the model adopted in [5], the equivalent circuit of the diode includes both the non linear junction and diffusion capacitances ($C_{di}(V_d)$ and $C_j(V_d)$) and the total current can be expressed as:

$$I_d = I_j + I_{C_{di}} + I_{C_j}$$

0-7803-4471-5/98/$10.00 (c) 1998 IEEE

with

$$I_j = I_0 \left(e^{\frac{q}{\eta K T} V_d} - 1 \right),$$

$$I_{C_{di}} = C_{di}(V_d) \frac{dV_d}{dt} \quad , \quad I_{C_j} = C_j(V_d) \frac{dV_d}{dt} \quad .$$

In the above equations K is the Boltzmann constant, T is the absolute temperature, I_0 is the inverse saturation current of the diode and η is the ideality factor that will be omitted in the rest of the discussion. The two non linear capacitances, in turn, are modeled by the following equations:

$$C_{di}(V_d) = \tau_d I_0 \frac{q}{KT} \left(e^{\frac{q}{KT} V_d} - 1 \right)$$

$$C_j(V_d) = C_j(0) \left(1 - \frac{V_d}{\phi_0} \right)^{-m} \qquad if\ V_d > F_c \phi_0$$

$$C_j(V_d) = \frac{C_j(0)}{F_2} \left(F_3 + \frac{m V_d}{\phi_0} \right)^{-m} \qquad if\ V_d \leq F_c \phi_0$$

where F_c, F_2, F_3 are suitable coefficients, m is the doping profile coefficient (usually 0.5 for abrupt junction), ϕ_0 is the built-in voltage and $C_j(0)$ is the static capacitance at $V_d = 0$.

The current equations are discretized in a similar way with the other lumped elements and two E-field transcedental equations are derived for $V_d < F_c \phi_0$ and $V_d \geq F_c \phi_0$. These equations can be solved in an iterative procedure (e.g. Newton-Raphson algorithm).

IV Applications of Nonlinear MRTD

The modeled Schottky GaAs diode has the following parameter values: $I_0 = 5.e-11\ A$, $\eta = 1.25$, $R_s = 13\,\Omega$, $C_j(0) = .29pF$, $\tau_d = 0$, $m = 0.5$, $F_c = .5$ For the analysis of the testing structure of Fig.(1), we have set up a mesh of $8 \times 30 \times 6$ cells with a cell size equal to $30 \times 60 \times 30\ \ \mu m$ ($60\ \mu m$ is $\lambda/10$ at about 135 GHz). The same structure has been also analyzed, for comparison, with FDTD method. This analysis has been performed by adopting two different meshes: the same mesh described before and a doubled mesh with the dimension: $16 \times 60 \times 12$ and $\lambda/10$ at about 270 GHz. The structure has been excited at the center with an impressed current source window. A sine-wave with a frequency of 45 GHz has been used, while a probe at the center of the structure has been considered. Figures (2),(3) and (4) show the results obtained with the coarse FDTD, the finer FDTD, and the MRTD respectively. The MRTD simulation has adopted the same mesh used in the coarsest FDTD analysis. The good agreement between the FDTD simulation with the fine mesh and the MRTD one, together with the fairly different results obtained with the coarse mesh FDTD analysis, put at the evidence the capability of the MRTD to better predict the frequency behavior of this non linear circuit. In particular, it is evident that with a coarse mesh, MRTD, in contrast to FDTD, can detect the harmonic null due to the location of the probe in the middle of the structure (in this position, in theory, no even harmonic mode should be detected).

Figure (5) shows the geometry of a stripline single-ended mixer, which is analyzed by use of MRTD. The used Schottky diode has the characteristics described above and is zero biased for simplicity. The LO and RF excitation signals have frequencies 43 GHz and 45 GHz and powers 20 dBm and -20 dBm respectively. The left (short-circuited) stub with length 900 μm is used as an IF signal block and the right (open-circuited) stub with length 1640 μm blocks the LO/RF signals at the output section. For this configuration, MRTD gives a conversion loss of -8.1 dB. LIBRA, a commercial EM simulator, calculates the conversion loss at -8.8 dB. In addition, (Table 1) shows that the relative output power of the harmonics gets similar values for MRTD and LIBRA simulations. These results emphasize the inherent capability of MRTD to describe efficiently the nonlinear elements, which create a discrete but infinite spectrum. Moreover, the MRTD allows for a time adaptive scheme which offers significant computational profit due to the iterative algorithm for the solution of the nonlinear equations. It has to be pointed out that LIBRA can give reliable results only for quasistatic geometries such as Figure (5). On the contrary, MRTD can simulate efficiently structures with multimodal propagation without the huge memory requirements of the conventional FDTD schemes.

0-7803-4471-5/98/$10.00 (c) 1998 IEEE

Table 1: Harmonics Power Distribution [dBm]

Freq [GHz]	2	41	43	45	88
LIBRA	-28.8	-56.1	-33.2	-40.1	-36.3
MRTD	-28.1	-54.7	-31.4	-38.2	-34.7

V Conclusion

An algorithm for the modeling of lumped elements with the MRTD scheme based on the Battle-Lemarie basis has been proposed and has been applied to the numerical analysis of a diode problem. The frequency spectrum has been calculated and verified by comparison to reference data. In comparison to Yee's conventional FDTD scheme, the proposed scheme offers memory savings by a factor of 2-6 per dimension maintaining a similar accuracy.

VI Acknowledgments

This work has been funded by NSF and ARO. The authors would like to thank Dr. F. Alimenti for the interesting and useful discussion about theoretical aspects concerning the multiresolution techniques and Prof. R. Sorrentino for the continuous support he gave to this work.

References

[1] M.Krumpholz, L.P.B.Katehi, "MRTD: New Time Domain Schemes Based on Multiresolution Analysis", IEEE Trans. Microwave Theory Tech., pp. 555-572, 1996.

[2] E.Tentzeris, M.Krumpholz and L.P.B. Katehi, "Application of MRTD to Printed Transmission Lines", Proc. MTT-S 1996, pp. 573-576.

[3] E.Tentzeris, R.Robertson, M.Krumpholz and L.P.B. Katehi, "Application of the PML Absorber to the MRTD Technique", Proc. AP-S 1996, pp. 634-637.

[4] W.Sui, D.Christensen and C.Durney, "Extending the two-dimensional FDTD Method to Hybrid Electromagnetic Systems with Active and Passive Lumped Elements", IEEE Trans. Microwave Theory Tech., pp. 724-730, 1992.

[5] G.Massobrio and P.Antognetti, "Semiconductor Device Modeling with Spice 2/E", McGraw-Hill.

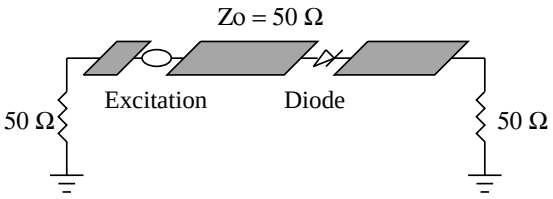

Figure 1: Diode Test Structure.

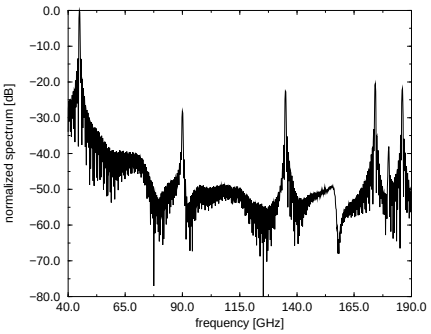

Figure 2: FDTD coarse mesh.

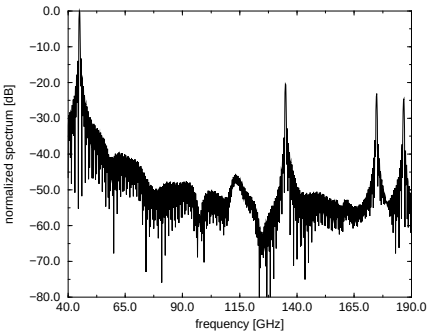

Figure 3: FDTD fine mesh.

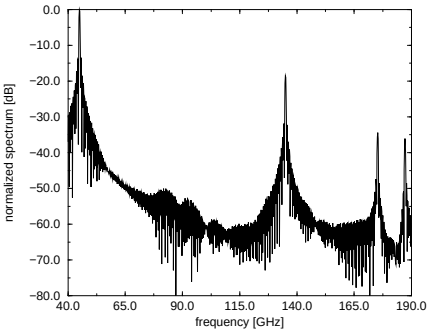

Figure 4: MRTD coarse mesh.

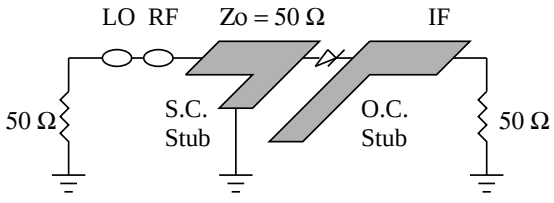

Figure 5: Mixer Geometry.